Chemisorption of H on Pd(111): An *ab initio* approach with ultrasoft pseudopotentials

W. Dong
Institut de Recherches sur la Catalyse, Centre National de la Recherche Scientifique, 2, Avenue Albert Einstein, F-69626 Villeurbanne Cedex, France
and Ecole Normale Supérieure de Lyon, 46, allée d'Italie, F-69364 Lyon Cedex 07, France

G. Kresse, J. Furthmüller, and J. Hafner
Institut für Theoretische Physik, Technische Universität Wien, Wiedner Hauptstrasse 8-10, A-1040 Wien, Austria
(Received 6 November 1995)

An *ab initio* study based on local-density-functional (LDF) theory is presented for the chemisorption of hydrogen on the Pd(111) surface. Our calculation uses the Vienna *ab initio* molecular-dynamics program (VAMP) based on (i) finite-temperature LDF, (ii) exact calculation of the electronic ground state and Hellmann-Feynman forces after each ionic move, and (iii) ultrasoft pseudopotentials for the electron-ion interaction. Complete geometry optimization for different adsorption sites are carried out. The energetic stability of the adsorption site correlates with the coordination number of the site. The larger the coordination number, the more stable the site. Both geometries and the electronic structure obtained from our theoretical calculations are in good agreement with experimental results. [S0163-1829(96)02924-4]

I. INTRODUCTION

In the last years, considerable progress has been made in quantum-mechanical *ab initio* calculations applied to material science.[1] The advances in this field come essentially from a few crucial ingredients: efficient calculation of the electronic ground state based on either the Car-Parrinello method[2] or conjugate-gradient techniques,[1,3–7] and the development of optimized first-principle pseudopotentials.[8–14] The efficiency of these methods has been quickly proven in the study of semiconductors (see Refs. 1 and 15–17 for reviews). However, metallic systems are more difficult to treat. There are several additional difficulties related to the characteristics of metals. The lack of an energy gap between the valence and conduction bands leads to a nonadiabaticity problem, and is a source of instability in the numerical methods. Transition metals have another particularity: the localized character of d electrons makes the norm-conserving pseudopotentials for these electrons very rapidly varying functions. This hampers seriously the efficiency of methods which use a plane-wave basis for expanding wave functions. The early remedy of this problem is to use a mixed basis consisting of plane waves and localized orbitals[18] or of a localized-orbital basis.[19] Vanderbilt proposed another approach, the so-called ultrasoft pseudopotential method.[20] Recent work[7,21–24] has shown that this approach opens very promising perspectives for extending *ab initio* studies to the ''problematic'' elements in the Periodic Table, i.e., first-row elements containing $2p$ electrons and transition metals.

In the present work, the chemisorption of hydrogen on a transition-metal surface P(111) is addressed by *ab initio* calculations with ultrasoft pseudopotentials. The study of the hydrogen-palladium system is both technologically and fundamentally important. The high ability of palladium to absorb hydrogen makes it a very good medium for hydrogen storage. In catalysis, e.g., Fischer-Tropsch hydrogenation reactions, palladium is a good catalyst. The dissociative adsorption of H_2 on palladium surface is the first elementary step of these reactions. Because of its importance, a large amount of work has been devoted to hydrogen-palladium systems by both experimental and theoretical approaches (see Refs. 25 and 26 for reviews). Much experimental information is now available for these systems. This makes them quite ideal candidates for thorough theoretical investigations. Low-energy electron-diffraction (LEED) measurements have been made for low-index clean palladium surfaces, e.g., Pd(111), Pd(110), and Pd(100) and for hydrogen adsorption on these surfaces.[27–31] By using thermal desorption spectroscopy (TDS), the energy of adsorption can be determined.[28] The change of the work function upon hydrogen adsorption can be measured at different coverage.[28,29] Combined with TDS, these measurements allow us to determine how the adsorption energy varies with the hydrogen coverage. While the compact (111) surface of palladium is not much perturbed by the adsorbate, experimental studies have shown that adsorbate-induced reconstruction can take place for the Pd(110) surface.[32] On the Pd(111) surface, some low-coverage ordered H phases are also observed experimentally, e.g., $p(\sqrt{3}\times\sqrt{3})R30°$ and $c(\sqrt{3}\times\sqrt{3})R30°$ patterns, as well as their order-disorder phase transitions.[33,34] The electronic structures of clean and hydrogen-covered palladium surfaces have been studied by means of ultraviolet photoelectron spectroscopy and electron-energy-loss spectroscopy.[35–39]

There are some theoretical studies of chemisorption of hydrogen on various palladium surfaces.[40–49] Early work was based on semiempirical approaches like embedded-atom[42] or embedded-cluster methods,[40,41] or the effective-medium model[43,50,51] which are all based on the same basic idea. Despite of their simplicity, these techniques are capable of describing the general features of hydrogen chemisorption on various transition metals. However, the application of these methods necessitates the fitting of some model parameters against experimental results. Theoretical investigations have been made also by modeling the surface

by finite size clusters.[48,49] It has been shown that some properties converge slowly with the system size.[52] A certain number of *ab initio* calculations for the chemisorption of hydrogen on some transition metals have also been carried out. Louie and co-workers have addressed a variety of interesting problems of hydrogen-palladium systems by using approaches based on pseudopotentials combined with either a mixed basis or a localized-orbital basis.[44–47] By using the linear augmented plane-wave method, Hamann made *ab initio* studies of adsorbate vibrations on transition-metal surfaces.[53] Very recently, *ab initio* calculations in a plane-wave basis of H_2 dissociation on noble-metal [Cu(111)],[54] transition-metal [Pd(100)],[55,56] and alloy surfaces [NiAl(110)] (Ref. 57) have been published. In these calculations, the electron-ion interaction is described by relatively hard norm-conserving pseudopotentials, leading to very high computational effort and convergence problems. It is therefore interesting to investigate the possibility to use ultrasoft pseudopotentials. Constrained by computational cost, most of the *ab initio* calculations up to now are carried out for high coverages, $\theta \geqslant 1$. While the results obtained from the studies in high-coverage cases furnish already valuable information, it is also desirable to be able to treat lower-coverage cases. It is believed that hydrogenation reactions take place at low hydrogen coverages, since there must be some adsorption sites left for the other reactants. Surface diffusion behavior also depends on the adsorbate concentration. Therefore, it is very useful to obtain also results for low adsorbate concentrations. In this paper, it will be shown that with the efficiency gained from recent progress in computational methods, we are now able to perform complete geometry optimizations for determining a quite detailed potential map of hydrogen chemisorbed on a Pd(111) surface at $\theta = \frac{1}{4}$.

Our theoretical approach is described in Sec. II. Results are presented in Sec. III along with discussions. Conclusions are summarized in Sec. IV.

II. THEORETICAL APPROACH

Our approach is based on density-functional theory[58,59] in the framework of the local-density approximation (LDA). We use the exchange-correlation functional determined by Ceperley and Alder.[60] In practice, it is the parametrization of Perdew and Zunger[61] for this functional which is implemented. To avoid the instability coming from the level crossing and quasidegeneracies in the vicinity of the Fermi level in metallic systems, fractional occupations of the eigenstates are allowed. This can be done by using finite-temperature local-density, functional theory where the free energy is the variational functional.[62] In this way, the Fermi surface can be smeared by Gaussian or Fermi-Dirac broadening. The technique of Methfessel and Paxton[63] for the Fermi-surface broadening also allows for an accurate calculation of Hellmann-Feynman forces. The k-space sampling is performed by using the special k points method proposed by Monkhorst and Pack.[64] The Kohn and Sham equation is solved numerically by a double-iteration procedure. First, a preconditioned conjugate-gradient method[4] is applied, for one band each time, to improve the eigenvalues and wave functions at a fixed potential. Once all the considered bands are swept, a subspace diagonalization among these bands is made. Then the Fermi energy, eigenlevel occupancies, charge density, and potential are updated using efficient mixing routines. The band-by-band minimization and the subspace diagonalization alternate until convergence is reached. The geometry optimization is carried out by using again the conjugate-gradient method. After each geometry update, an extrapolation of wave functions is made to improve the input for the next step. The electron-ion interaction is modeled by pseudopotentials. Optimized nonlocal ultrasoft pseudopotentials are used. The pseudopotential optimization procedure has been described elsewhere.[14] For systems of large size, e.g., more than 15 atoms, the real-space projection technique proposed by King-Smith, Payne, and Lin[65] to handle the nonlocal part of the pseudopotential furnishes a considerable gain in computational efficiency. All the above features of the computation techniques are implemented in the recently developed Vienna *ab initio* molecular-dynamics program (VAMP). A more detailed description of the program can be found in the paper by Kresse and Hafner.[66] This approach has been applied successfully to a variety of problems in condensed-matter physics.[7,66–70]

III. RESULTS AND DISCUSSIONS

A. Pseudopotentials

In our approach, the electron-ion interaction is described by pseudopotentials. The norm-conserving concept introduced by Hamann, Schlüter, and Chiang[8] plays a central role in constructing modern pseudopotentials.[8–14] With the help of the Friedel sum rule, it can be shown that the norm-conserving condition improves the transferability of the pseudopotential. While the norm-conserving requirement assures the highly desirable transferability, at the same time it imposes a quite rigid constraint on the pseudo-wave-functions. It is now well known that the norm-conserving pseudopotentials for transition metals are relatively ''hard.'' Consequently, the basis size will be very large if the wave functions are expanded in plane waves. Thus the study of large systems, e.g., solid surfaces modeled by a slab supercell, can become almost impossible computationally. The so-called ultrasoft pseudopotentials were recently proposed by Vanderbilt[20] to reconcile these conflicting aspects: accuracy, transferability, and plane-wave convergence. In this method, short-range augmentation functions are introduced for describing the charge density, and the norm-conserving requirement is no longer applied uniquely to the pseudo-wave-functions but to the augmentation functions and the pseudo-wave-functions together. This allows us to generate very soft pseudopotentials, and to use a much lower cutoff energy for the plane-wave expansion than in the case of the usual norm-conserving pseudopotentials. The augmentation functions are defined as

$$Q_{ij}(\mathbf{r}) = \phi_i^{\mathrm{AE}}(\mathbf{r})\,\phi_j^{\mathrm{AE}}(\mathbf{r}) - \phi_i^{\mathrm{ps}}(\mathbf{r})\,\phi_j^{\mathrm{ps}}(\mathbf{r}), \tag{1}$$

where $\phi^{\mathrm{AE}}(\mathbf{r})$ and $\phi^{\mathrm{ps}}(\mathbf{r})$, respectively, are all-electron and pseudo-wave-functions. In practice, $\phi^{\mathrm{AE}}(\mathbf{r})$ is pseudized by using a high-quality norm-conserving pseudo-wave-function. In the ultrasoft pseudopotential method introduced by Vanderbilt, several reference energies can also be included. In this work, an ultrasoft pseudopotential for palladium has been generated from the reference electron configuration

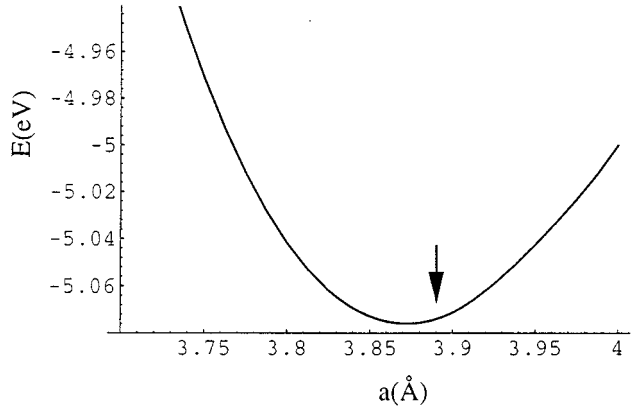

FIG. 1. Cohesive energy as a function of the lattice constant for bulk Pd. The arrow indicates the experimental value of the lattice constant.

$4d^9 5s^1 5p^0$. For s and p components, norm-conserving pseudopotentials are constructed at the following cutoff radii and reference energies: $R_{c,s}=1.1113$ Å and $R_{c,p}=1.4288$ Å, and $\epsilon_s=-4.63$ eV and $\epsilon_p=-1.36$ eV. For the d component, an ultrasoft pseudopotential is generated at two reference energies: $\epsilon_{d,1}=-6.93$ eV and $\epsilon_{d,2}=-8.16$ eV with a cutoff radius $R_{c,d}=1.4288$ Å. The pseudized augmentation function is generated at the same reference energies with a cutoff radius of 1.0584 Å. The ultrasoft pseudopotential of hydrogen is generated from the reference electron configuration $1s^1 2p^0$ at $R_0=0.6615$ Å with reference energies $\epsilon_{s,1}=-6.36$ eV, $\epsilon_{s,2}=-9.52$ eV, and $\epsilon_p=-3.40$ eV. The pseudized augmentation function is generated with a cutoff radius equal to 0.4233 Å. For a more detailed discussion of the ultrasoft pseudopotentials and all technical aspects, we refer the interested reader to the paper by Kresse and Hafner.[14]

B. Bulk palladium

In the present work, plane waves with a cutoff energy equal to 200 eV are used to expand wave functions. The special points method proposed by Monkhorst and Pack[64] is applied to carry out the Brillouin-zone integrations. For bulk face-centered-cubic Pd, a $9\times9\times9$ grid is used for k-space sampling. Gaussian smearing with a width $\delta=0.4$ eV is used for the fractional occupancy of eigenlevels. The result corresponding to the zero temperature can be obtained by taking the limit $\delta\rightarrow0$ analytically.[71] The variation of the cohesive energy with the lattice constant is shown in Fig. 1. From this plot, we find the equilibrium lattice constant, $a=3.876$ Å, in excellent agreement with the experimental value 3.89 Å.[72] The bulk modulus $B_T=2.25\times10^{12}$ dyn/cm^2 agrees reasonably well with the measured value $B_T=1.81\times10^{12}$ dyn/cm^2,[72] and the theoretical value $B_T=2.15\times10^{12}$ dyn/cm^2 reported by Tomanek, Sun, and Louie[47] using the Hedin-Lundquist exchange, correlation functional. However, the cohesive energy is overestimated by 30%, i.e., E(theory) $=5.07$ eV and E(experiment)$=3.89$ eV. This overbinding, manifested in the cohesive energy and the bulk modulus, is a characteristic failure of the LDA and must be attributed to the nonlocal contribution to the exchange-correlation energy.

C. Clean Pd(111) surface

For the study of surfaces, we adopt the slab supercell approach. The solid slabs are separated by a vacuum layer corresponding to five ideal bulk palladium layers. This is a sufficiently large distance to avoid the interaction between the slab and its periodic images. Test calculations are carried out for several slab thicknesses: five, seven, and nine Pd layers (always with a five-layer vacuum). The difference between the surface energies obtained for five- and nine-layer slabs is only 26 meV/atom. Hence a five-layer system is sufficient for energetics. Here the Brillouin-zone integration is made on a $9\times9\times1$ grid of Monkhorst-Pack special k points. The surface energy is defined as

$$\sigma=(E_{\text{slab}}-N_{\text{atom}}E_{\text{bulk}})/2, \tag{2}$$

where E_{slab} is the total energy of the slab, E_{bulk} the total energy of the bulk crystal per atom, and N_{atom} the number of atoms in the slab. We find 0.75 eV/atom for the five Pd layers and five vacuum layers system. Recently, Methfessel, Hennig, and Scheffler made a systematic study of $4d$ transition-metal surfaces using the full-potential linear-muffin-tin-orbital (LMTO) method.[73] They have obtained 0.68 eV/atom for a Pd(111) surface with a seven-layer slab. Our result agrees well with the full-potential LMTO result.

Since VAMP allows for an analytical calculation of the forces, a geometry optimization can be readily carried out. This provides the possibility to make thorough study of surface relaxations. For the Pd(111) surface, we find that there is no relaxation. This agrees well with experimental results.[30] In contrast to surfaces having more open structures like Pd(110) or Pd(100), the compact Pd(111) surface undergoes a very small relaxation, if there is any. In the work of Methfessel, Hennig, and Scheffler,[73] an extremely small inward relaxation of 0.1% is reported.

The local density of states (DOS) is a very helpful tool for examining the reorganization of electronic structure when a surface is formed. We define the local DOS by

$$D(E,\mathbf{r}_a)=\sum_i \int d\mathbf{r}\,\theta(R-|\mathbf{r}-\mathbf{r}_a|)\,\psi_i^*(\mathbf{r})\,\psi_i(\mathbf{r})\,f(E-E_i), \tag{3}$$

where $\mathbf{r}_a$ is the position of the atom around which local DOS is calculated, $\theta(x)$ is the Heaviside function, and $\theta(R-|\mathbf{r}-\mathbf{r}_a|)$ delineates a sphere of radius R around $\mathbf{r}_a$. Throughout this work, we use the Wigner-Seitz radius for R. The index i is a compact notation of all quantum numbers which specify the wave functions. The summation over i includes the Brillouin-zone integration as well as the summation over bands. $f(E-E_i)$ is the fractional occupancy of the level E_i. In this work, we use the first-order expression of Methfessel and Paxton for $f(E-E_i)$.[63] In Fig. 2, the local DOS for the first four layers of a nine-layer slab is presented. The local DOS on the fourth-layer atom is essentially the same as the bulk DOS. It can be seen clearly that the perturbation does not go deeper than three layers. For the atom on the surface layer, the eigenstates near the Fermi level are more populated. This reflects the broken bonds of the surface atoms, and the resulting increase in the energy of the bonding state. Louie has studied the electronic structure of Pd(111) surface by using a pseudopotential method based on

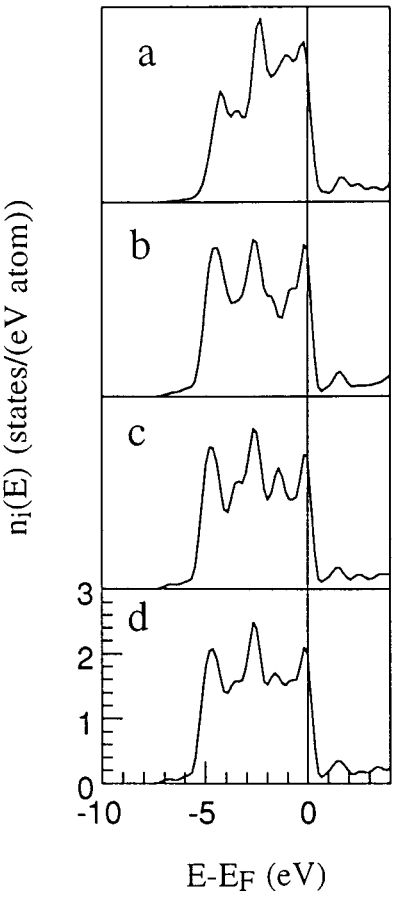

FIG. 2. Local densities of states $n_i(E)$ for clean Pd(111): (a) first layer, (b) second layer, (c) third layer, and (d) fourth layer.

a mixed basis.[44] Our result compares well with his result. Recently, Eichler *et al.*[69] carried out *ab initio* calculations for rhodium surfaces. The comparison between the present work and that of Eichler *et al.* shows that many similarities can be found between Pd(111) and Rh(111).

It is well known that some localization of electrons takes place near a solid surface. This leads to the so-called surface states. These surface states characterize the surface chemical reactivity since they are involved in most surface chemical reactions. Surface states can be determined by examining the degree of localization of wave functions on surface layers. In this work, the top and the first subsurface layers are taken as surface layers. Hence there are four layers being considered as surface layers for a slab, two on each side. While a five-layer slab is sufficient to obtain results for the energetics, a nine-layer slab is necessary for properly determining the band structure of surface states. Such a band structure for the clean Pd(111) surface is presented in Fig. 3 along with the bulk Pd band structure projected on the surface Brillouin zone. For determining the surface states given in Fig. 3, we have used a criterion of 90% and 75% localization of wave functions in the surface layers to define surface states. The darker points in this figure correspond to more localized states. The surface-state band structure of Pd(111) has also been determined by Louie,[44] but the way in which the surface states are characterized was not described. The surface band structure we have found with the criterion given above

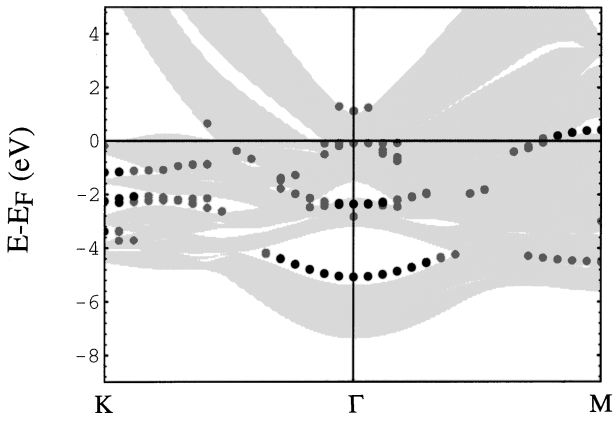

FIG. 3. Surface band structure for clean Pd(111). The shaded zone is the band structure of the bulk projected onto the (111) surface Brillouin zone. Surface states are presented by dots: darker dots present states with 90% localization, brighter dots states with 75% localization in the two top layers. Energies are measured relative to the Fermi level.

TABLE I. Surface states on clean Pd(111).

		Theoretical energy (eV)		
Symmetry points	Experimental energy[a] (eV)	Ultrasoft pseudopotential[b]	Norm-conserving pseudopotential[a]	LCAO[c]
Γ	>-0.3	-0.1	-0.2	-0.07
	-2.2	-2.3	-2.0	-2.28
		-4.9		
K	>-0.3	-0.2	-1.0	-0.49
		-1.2		
	-2.1	-2.3	-1.9	-1.44
		-3.4		
M	-1.0	-3.0	-3.8	-4.16
		-4.5		

[a]Eberhardt and co-workers, Refs. 37 and 38.
[b]Present work.
[c]Bisi and Calandra, Ref. 74.

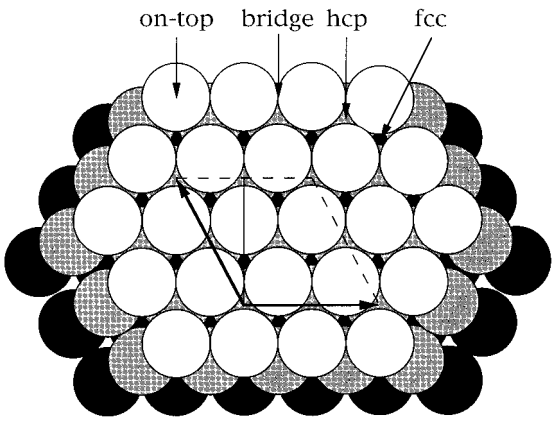

FIG. 4. Schematic presentation of a (111) surface and the different adsorption sites of high symmetry. The arrows represent the basis vectors of the (2×2) surface unit cell, the vertical line the path along which the adsorption energies have been calculated.

has the same general features as that determined by Louie, apart from some details concerning mainly the projected bulk band structure. A surface band structure can be determined experimentally by angle-resolved photoelectron spectroscopy. Experimental results obtained with this technique have been published by Eberhardt and co-workers[37,38] for a clean Pd(111) surface, and for H/Pd(111). The comparison between our results, experimental measurements, and two other theoretical results is given in Table I for a few special symmetry points in k space. There is a very good agreement between our results and the experimental ones.

D. Hydrogen adsorption on the Pd(111) surface

In this work, the ultrasoft pseudopotential is used also for hydrogen. Technical details concerning the construction of this pseudopotential have been given at the beginning of this section. With the ultrasoft pseudopotential some properties of the hydrogen molecule H_2 have been calculated. We obtain 0.765 Å for the bond length, in good agreement with the experimental value of 0.74 Å. For the total energy of H_2, we find -30.73 eV when a cutoff energy $E_{\text{cut}}=200$ eV is used for the expansion of wave functions. Due to the particularity of the hydrogen atom which has only one electron, the experimental value of the total energy of H_2, -31.66 eV, can be obtained from the experimental results of the ionization potential of the hydrogen atom and the dissociation energy of H_2. Our calculated value is of an error about 3%. The effect of this error on the adsorption energy will be discussed below.

Now, let us see first the results for monolayer coverage [$\theta=1$, (1×1) surface geometry]. At this coverage, several high-symmetry adsorption sites are studied. In Fig. 4, a top view of the Pd(111) surface is given, where the high-symmetry adsorption sites are indicated. There are two types of threefold sites: one called the fcc site, the other the hcp site. The difference between them is that there is a palladium atom below the hcp site in the second layer and below the fcc site in the third layer (i.e., an adatom placed at the fcc site continues the bulk lattice).

The calculations of the energetics and the geometry optimizations are carried out on asymmetric slabs, i.e., five Pd layers and a five-layer vacuum with H adsorbed on one side. The adsorption energy can be defined by

$$E_{\text{ad}}=E[\text{Pd}(111)]+E(\text{H}_2)/2-E[\text{H/Pd}(111)]. \qquad (4)$$

The results for adsorption energies and the optimized geometries are summarized in Table II. The results given in Table II are obtained from complete geometry optimizations, i.e., Pd atoms are also allowed to relax. For these high-symmetry sites, the H-induced relaxation is extremely small. The threefold sites are the most stable, and the fcc site is slightly more stable than the hcp site. It can be noted that the adsorption energy increases with the coordination number of the adsorbates, i.e., the on-top site is the least stable one, and the bridge site has an intermediate value of adsorption energy. The adsorption energy as defined in Eq. (4) can be measured by a thermal desorption method. Using this technique Conrad, Ertl, and Latta[28] have found $E_{\text{ad}}=0.45$ eV/atom for the adsorption energy of H on a Pd(111) surface at very low coverages. Our theoretical result for the fcc site overestimates the adsorption energy by 0.44 eV compared to the experimental value. Since the adsorption energy here is quite a small quantity, it is particularly hard to determine it accurately from the subtraction of several large numbers. As we have seen, there is a relative error of 3% in the calculation of the energy of H_2. Although this is not a large relative error, the absolute error is 0.93 eV. This can have quite a large effect on the results for the adsorption energy. In Table II,

TABLE II. Adsorption energy E_{ad} and adsorption site geometries.

		fcc site	hcp site	bridge site	on-top site
E_{ad} (eV)	experiment[a]	0.45			
	theory $\theta=1$	0.890(0.425)[b]	0.830(0.365)	0.691(0.226)	0.301(−0.164)
	$\theta=1/4$	1.153(0.688)	1.117(0.652)	0.870(0.405)	0.478(0.013)
H-metal spacing (Å)	experiment[c]	0.85±0.05	0.80±0.05	1.0±0.1	1.4±0.1
	theory $\theta=1$	0.86	0.86	1.03	1.55
	$\theta=1/4$	0.81	0.82	0.98	1.54

[a]Christmann, Ertl, and Schober, Ref. 27.

[b]The number in parentheses gives the adsorption energy corrected for the LDA error in the binding energy of the H_2 molecule.

[c]Felter, Sowa, and van Hove, Ref. 31.

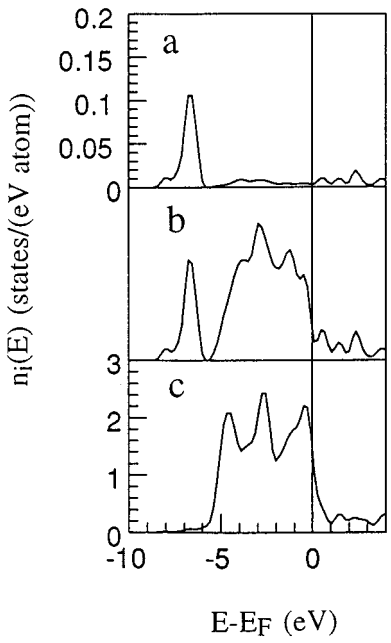

FIG. 5. Local densities of states $n_i(E)$ for H/Pd(111) at $\theta=1$ (monolayer coverage): (a) H on the fcc site, (b) first Pd layer, and (c) second Pd layer.

we also give results for the adsorption energy obtained by correcting the 3% error in the energy of H_2. These results are put in parentheses. We see now that the results for the three-fold sites compare much better with the experimental result. Hence the error in the binding energy of H_2 is the main source of errors in the adsorption energy calculations. This is a result characteristic for the LDA. A variety of high symmetry adsorption site geometries have been determined by Felter, Sowa, and van Hove[31] by fitting the LEED intensity-voltage curves. Some of their results for metal-H spacing are also listed in Table II. Here the metal-H spacing is defined as the distance between the H atom and the plane of the first-layer surface atoms. Our results are in very good agreement with their results.

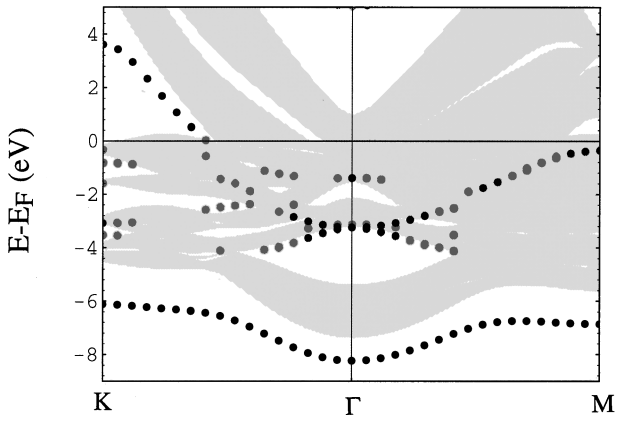

FIG. 6. Surface band structure for H/Pd(111), H on fcc site, and $\theta=1$. The shaded zone is the band structure of the bulk projected onto the (111) surface Brillouin zone. Surface states are presented by dots: darker dots present 90% localization and brighter dots 75% localization in the H layer and the two top Pd layers.

TABLE III. Surface states of H/Pd(111) (monolayer coverage).

		Theoretical energy (eV)	
Symmetry Points	Experimental energy[a] (eV)	Ultrasoft pseudopotential	Norm-conserving pseudopotential[b]
Γ	−1.2	−1.4	−1.3
	−3.1	−3.2	−3.2
	−7.9	−8.2	−7.5
K		−0.3	
	−1.0	−0.8	−0.8
		−1.6	
	−2.8	−3.0	−2.8
		−3.5	
	−5.9	−6.1	−6.3
M	−4.1	−0.4	−0.6
	−6.4	−6.8	−6.8

[a]Eberhardt and co-workers, Refs. 37 and 38.
[b]Present work.

Figure 5 shows the local DOS for hydrogen on the fcc site, as well the DOS's for the first and second palladium layers. The most salient feature here is that a split-off peak appears in the local DOS on the first Pd layer. A concomitant change in this local DOS is the depletion of levels near the Fermi level. This indicates clearly the participation of these levels in forming the chemisorption H-Pd bond. From Fig. 5, one can also observe that the H-Pd bond is quite localized. The local DOS on the second layer is almost unmodified compared to that of the clean surface (see Fig. 2). Hence only the nearest neighbors are directly involved in the chemisorption bond formation. This is why there is almost no difference between the results for fcc and hcp sites. The ultraviolet photoelectron spectra of H/Pd(111) have been obtained experimentally by Conrad *et al.*[35] and Demuth[36] independently. The experimental value for the position of the hydrogen-induced split-off peak is 6.5 eV below the Fermi level. Our result of 6.55 eV below E_F is in excellent agreement with experiment.

In Fig. 6, the surface-state band structure is presented for H on the fcc site. The band-structure calculation presented in this figure is made with a symmetric slab consisting of nine Pd layers and two H atoms, one on each side. The lowest band is the H-induced band which has a bandwidth of about 2.0 eV. Again, we see that this state is a very localized one, i.e., 90% localization on surface layers. The experimental determination of the band structure has been published by Eberhardt and co-workers,[37,38] and theoretical calculations by Louie[45] and Bisi and Calandra.[74] A very good agreement is observed again between our result, the experimental one and the previous theoretical results. In Table III, the comparison is made at some special points of the surface Brillouin zone.

In this work, we have also studied hydrogen chemisorption at a lower coverage, i.e., $\theta=1/4$. As we have mentioned in Sec. I, hydrogenation reactions take place at low hydrogen coverages. Some sites must be unoccupied by H and remain accessible for the other reactant. Therefore, it is also important to study the low-coverage cases. For this purpose, a (2×2) supercell is considered. Now each layer contains four

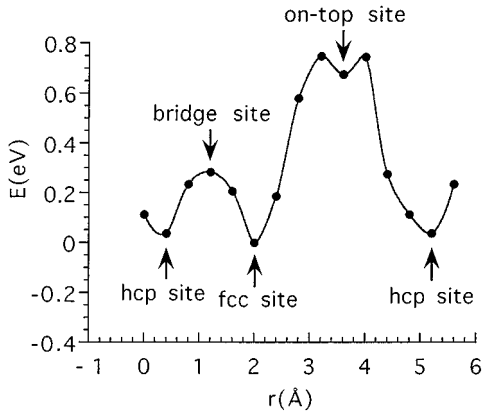

FIG. 7. Potential-energy profile for a hydrogen atom on a Pd(111) surface calculated along the path sketched in Fig. 4. The coverage is $\frac{1}{4}$ of a monolayer ($\theta=0.25$).

palladium atoms. The energetics and geometry optimizations are again made on the asymmetric slab consisting of five Pd layers and one adsorbate layer. A symmetric slab of nine Pd layers and H layers on both sides is used for the band-structure calculation, always with a vacuum corresponding to five ideal bulk Pd layers. This symmetric slab contains a total of 36 Pd atoms. All calculations for the (2×2) supercell are made with a $3\times3\times1$ Monkhorst-Pack grid for k-space sampling.

The geometries of high-symmetry adsorption sites and the adsorption energies are summarized in Table II together with the results for $\theta=1$. The ordering of the site stabilities remains the same as for $\theta=1$. From Table II, one can see that the adsorption energies for all the sites increase when the surface concentration of the adsorbate is decreased. This implies that the adsorbate-adsorbate interaction is of a repulsive character. Even at $\theta=1$, the H-H distance is already sufficiently large so that the direct H-H interaction is weak. Hence the lateral H-H interaction is mediated by the surface palladium atoms, i.e., so-called through-bond interactions.

Besides the high-symmetry adsorption sites discussed above, we have also carried out calculations for some additional points on the path which connects the high-symmetry sites. Such a path is indicated in Fig. 4 by the vertical line in the (2×2) cell. The minimum-energy profile along this path is presented in Fig. 7. To determine this profile, the x and y coordinates of the adsorbate are held fixed at a chosen point on the path, and the height of the adsorbate is optimized to minimize energy. During this optimization, the positions of the Pd atoms in the first three layers are also allowed to relax. We see, from Fig. 7, that the two threefold sites of different types are separated by an energy barrier of 0.28 eV. The saddle point is situated at the bridge site. This is a quite moderate energy barrier. Hence hopping of the adsorbed hydrogen between the threefold sites can take place rapidly. A somehow surprising result is that the on-top site is not an energy maximum but a local minimum. The barrier between the fcc site and the on-top site amounts to 0.75 eV. Therefore, the surface diffusion of the hydrogen at low temperatures takes place by doing zigzag hoppings between the threefold sites.

In the calculations made to obtain the energy profile given in Fig. 7, complete geometry optimizations are performed for the palladium atoms in the slab. The positions of Pd atoms are allowed to adjust themselves when the hydrogen atom is displaced along the path. On the section between the two threefold sites which passes through the bridge site, no geometry change of palladium atoms is found. However, on the section connecting the fcc site to the on-top site and that between the hcp and on-top sites, some quite large displacements of palladium atoms are found. To be concrete, let us describe what we have observed for the section connecting the hcp site to the on-top site. Up to the middle point between the hcp and the on-top site, the first-layer palladium atoms undergo a displacement parallel to the surface which follows the displacement of the hydrogen. After the middle point, no such displacement of palladium atoms is observed. What happens when the hydrogen atom is displaced from the fcc site toward the on-top site is very similar. We can understand this geometry change in the following way. If the positions of the Pd atoms are kept fixed, the coordination number of the hydrogen atom changes from 3 to 1 when it is displaced from a threefold site toward the on-top site. Due to the weakening of H-Pd interaction related to the decrease of the coordination number of the hydrogen, the energy of the system increases. If a displacement of neighboring Pd atoms following the hydrogen displacement can occur, the local environment of the hydrogen with a threefold site is more or less recovered. In this way, energetic stability can be improved on one hand, but on the other hand the distortion of Pd-Pd bonds between the first and the second layers increases the system energy. Therefore, the final optimized geometry results from the balance of these two factors. When the hydrogen is placed halfway between the hcp and on-top sites, the first Pd layer undergoes a displacement of 0.5 Å in the direction of the hydrogen displacement, and the second Pd layer a displacement of 0.2 Å in the same direction. This geometric deformation of the surface does not go deeper into the bulk. After the midpoint, the displacement of the Pd layer needed to even partially recover the local threefold environment would become large. The resulting large distortion of the Pd-Pd bond between the first and second layers makes such a displacement very unfavorable. This is why no surface layer displacement is found between the midpoint and the on-top site. A very similar argument can be developed to understand why there is no Pd-layer displacement when the hydrogen atom is displaced from the hcp site to the fcc site via the bridge site. Here the situation is a bit different. Over all this section, the coordination number of the hydrogen is never reduced to less than 2. Hence the stability gained from the local environment recovering is smaller, which cannot compensate for the energy rise from the Pd-Pd bond distortion. Therefore, there is no displacement of the palladium surface layer in this case.

In Fig. 8, the local DOS's on the hydrogen atom and the Pd atoms on the surface layer are presented for the adsorption on the fcc, bridge, and on-top sites. Substantial modification is found only on the atoms directly involved in chemisorption bonding. Hence the split-off peak appears on three Pd atoms in the case of the fcc site and only on two Pd atoms in the bridge-site case. There is no split-off peak in the case of the on-top site. As the coordination number decreases, the adsorbate-substrate interaction decreases. As a consequence, the H-Pd bonding level is raised in energy. From Fig. 8, we

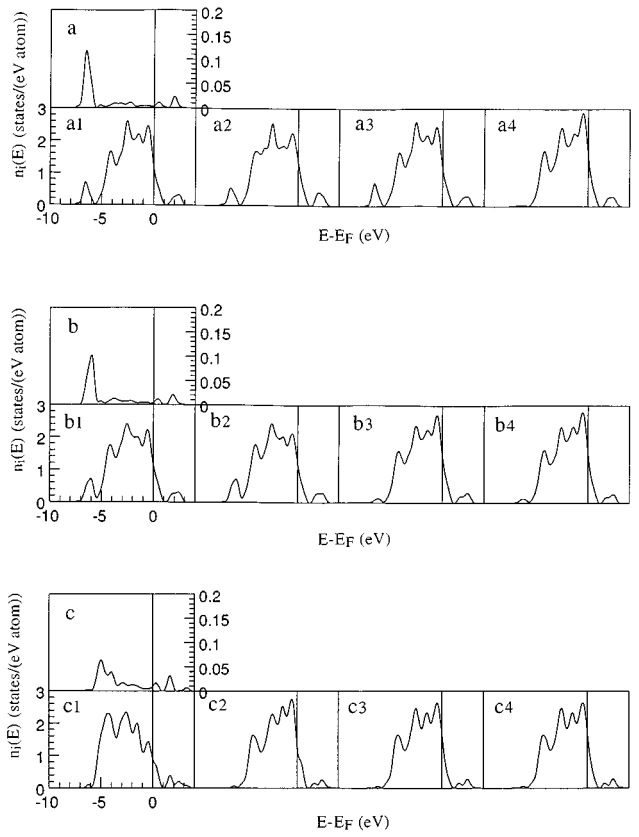

FIG. 8. Local densities of states $n_i(E)$ for H/Pd(111), $\theta=1/4$: (a) H on the fcc site and (2×2) cell, (b) H on the hcp site, and (c) H on the on-top site. In each panel the top figure represents the DOS on the H atom, and the lower panels labeled 1–4 are the DOS on the four inequivalent Pd atoms in the (2×2) cell.

see clearly that the split-off peak is shifted toward the Fermi level as the coordination number of the adsorbate decreases. This shift is so large in the case of the on-top site that the H-Pd bonding level is no longer characterized by a split-off peak. Only the shoulder at the bottom of the *d* band indicates the presence of the H-Pd bonding level in this region.

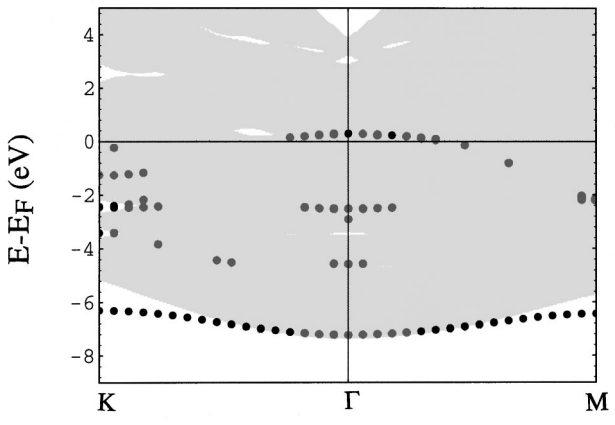

FIG. 9. Surface band structure for H/Pd(111), H on the fcc site, and $\theta=\frac{1}{4}$. The shaded zone is the band structure of the bulk projected onto the (111) surface Brillouin zone. Surface states are presented by dots: darker dots present 90% localization in the H and the two top Pd layers, and brighter dots 75% localization.

The surface-state band structure for the (2×2) supercell is shown in Fig. 9 for the case of the H atom at the fcc site. When the size of the unit cell is increased, the Brillouin zone shrinks. Due to the band folding resulting from the Brillouin-zone shrinking, the projected bulk band structure has a different appearance from that shown in Fig. 6 for a (1×1) unit cell. Here we again observe a very localized surface state resulting from H-Pd bonding. The width of this band is reduced compared to that in the case of $\theta=1$ shown in Fig. 6. The decrease of the bandwidth is due to the larger distances between the hydrogen atoms at low coverage.

IV. CONCLUSIONS

In this paper, we have shown that recent advances in computational techniques now allow one to perform very detailed *ab initio* studies of chemisorption on transition metals. The ultrasoft pseudopotential is a very efficient method to treat the quite localized *d* electrons. Electron localization in surface states and adsorbate-substrate bonds is adequately described. The use of ultrasoft pseudopotentials allows us to expand the wave functions in a basis of plane waves even in the case of transition metals. One important advantage of the plane-wave expansion is to allow for an analytic calculation of the Hellmann-Feynman forces. This greatly facilitates the geometry optimization.

For the chemisorption of hydrogen on Pd(111), we find that the adsorbate-substrate bonding energy correlates with the coordination number of the adsorption site. The threefold sites, i.e., fcc and hcp sites, are the most stable ones. Due to the localized feature of the adsorbate-surface bonding, the fcc and hcp sites have very similar stabilities. They are separated by a moderate energy barrier ($\Delta E=0.28$ eV for $\theta=\frac{1}{4}$) via the twofold bridge site. The on-top site is the least stable. Nevertheless, it corresponds to a local-energy minimum. The energy barrier between a threefold site and the on-top site is much higher than that between the two threefold sites via the bridge site. Hence it can be inferred that the diffusion of the hydrogen on the surface takes place essentially by zigzag hopping among the threefold sites.

The optimized geometries of different adsorption sites agree well with the experimental results by LEED. The electronic structure is also determined accurately by our approach. The calculated surface band structures for both clean Pd(111) and H/Pd(111) are in good agreement with the experimental results obtained from angular-momentum-resolved photoelectron spectroscopy. The most salient modification of electronic structure by chemisorption is the appearance of a split-off peak in the eigenvalue spectrum. There is an excellent agreement between our calculation and the experimental result for the position of the split-off peak. Although some overestimation of cohesive and adsorption energies due to the local-density approximation is found, our theoretical approach gives an overall satisfactory description of chemisorption on transition-metal surfaces. This opens very attractive perspectives for the study of elementary chemical processes at surfaces.

An important point to be emphasized is that although the chemisorption of H on Pd(111) has been previously studied at monolayer coverage, our results are the first for a surface coverage as low as $\theta=\frac{1}{4}$. This is made possible by the effi-

ciency of our technique, which allows us to study a large (2×2) surface cell for a relatively thick slab of five layers. In comparison with the monolayer coverage, we find that at $\theta=\frac{1}{4}$ the energetic preference of the fcc site over the other high-symmetry adsorption sites is reduced for the hcp site, but increased for the bridge and on-top sites (cf. Table II). The increase of the energy barrier for the migration between fcc and hcp sites at reduced coverage is a useful piece of information for studying adsorbate diffusion. We also find that the reduced coverage leads to a lower equilibrium adsorption height of the H atom (by about 0.05 Å). We have also studied in detail the changes in the surface electronic structure at reduced coverage. In particular, we find that the amplitude of the H-induced splitting from the Pd conduction band is reduced, and that at lower coverage the H-induced depletion near the Fermi level is strongly reduced (cf. Figs. 5 and 8). We would expect that the changes in the DOS near the Fermi energy reflects some change in the chemical reactivity of the surface.

ACKNOWLEDGMENTS

Computer time on Cray C98 has been allocated for the present work by IDRIS du Centre National de la Recherche Scientifique through Project No. 950609. Work at the Technische Universität Wien has been supported by the Bundes Ministerium für Wissenschaft und Forschung through the Center for Computational Material Science. Bilateral cooperation has been supported within the framework of the Austro-French Agreement on Scientific and Technical Cooperation (Project No. 95.44.13).

[1] M. C. Payne, M. P. Teter, D. C. Allan, T. A. Arias, and J. D. Joannopoulos, Rev. Mod. Phys. **64**, 1045 (1992).
[2] R. Car and M. Parrinello, Phys. Rev. Lett. **55**, 2471 (1985).
[3] M. J. Gillan, J. Phys. Condens. Matter **1**, 689 (1989).
[4] M. P. Teter, M. C. Payne, and D. C. Allan, Phys. Rev. B **40**, 12 255 (1989).
[5] J. Stich, R. Car, M. Parrinello, and S. Baroni, Phys. Rev. B **39**, 4997 (1989).
[6] G. Kresse and J. Hafner, Phys. Rev. B **47**, 558 (1993).
[7] G. Kresse and J. Hafner, Phys. Rev. B **48**, 13 115 (1993).
[8] D. R. Hamann, M. Schlüter, and C. Chiang, Phys. Rev. Lett. **43**, 1494 (1979).
[9] G. B. Bachelet, H. S. Greenside, G. A. Baraff, and M. Schlüter, Phys. Rev. B **24**, 4745 (1981).
[10] G. B. Bachelet, D. R. Hamann, and M. Schlüter, Phys. Rev. B **26**, 4199 (1982).
[11] D. Vanderbilt, Phys. Rev. B **32**, 8412 (1985).
[12] A. M. Rappe, K. M. Rabe, E. Kaxiras, and J. D. Joannopoulos, Phys. Rev. B **41**, 1227 (1990).
[13] N. Troullier and J. L. Martins, Phys. Rev. B **43**, 1993 (1991).
[14] G. Kresse and J. Hafner, J. Phys. Condens. Matter **6**, 8245 (1994).
[15] W. E. Pickett, Comput. Phys. Rep. **9**, 115 (1989).
[16] G. P. Srivastava and D. Weaire, Adv. Phys. **36**, 463 (1987).
[17] M. L. Cohen and J. R. Chelikowsky, *Electronic Structure and Optical Properties of Semiconductors*, 2nd ed., Springer Series in Solid-State Sciences Vol. 75 (Springer-Verlag, Berlin, 1989).
[18] S. G. Louie, K. M. Ho, and M. L. Cohen, Phys. Rev. B **19**, 1774 (1979).
[19] C. T. Chan, D. Vanderbilt, and S. G. Louie, Phys. Rev. B **33**, 2455 (1986).
[20] D. Vanderbilt, Phys. Rev. B **41**, 7892 (1990).
[21] A. Pasquarelleo, K. Laasonen, R. Car, C. Lee, and D. Vanderbilt, Phys. Rev. Lett. **69**, 1982 (1992).
[22] K. Laasonen, R. Car, C. Lee, and D. Vanderbilt, Phys. Rev. B **43**, 6796 (1991).
[23] K. Laasonen, A. Pasquarello, R. Car, C. Lee, and D. Vanderbilt, Phys. Rev. B **47**, 10 142 (1993).
[24] K. Laasonen, M. Sprik, M. Parrinello, and R. Car, J. Chem. Phys. **99**, 9080 (1993).
[25] See, e.g., *Hydrogen in Metals I and II*, edited by G. Alefeld and J. Völkl, Topics in Applied Physics Vols. 28 and 29 (Springer-Verlag, Berlin, 1978).
[26] K. Christmann, Surf. Sci. Rep. **9**, 1 (1988).
[27] K. Christmann, G. Ertl, and D. Schober, Surf. Sci. **40**, 61 (1973).
[28] H. Conrad, G. Ertl, and E. E. Latta, Surf. Sci. **41**, 435 (1974).
[29] M. G. Cattania, V. Penka, R. J. Behm, K. Christmann, and G. Ertl, Surf. Sci. **126**, 382 (1983).
[30] H. Ohtani, M. A. Van Hove, and G. A. Somorjai, Surf. Sci. **187**, 372 (1987).
[31] T. E. Felter, E. G. Sowa, and M. A. Van Hove, Phys. Rev. B **40**, 891 (1989).
[32] C. J. Barnes, M. Q. Ding, M. Lindroos, R. D. Diehl, and D. A. King, Surf. Sci. **162**, 59 (1985).
[33] T. E. Felter and R. H. Stulen, J. Vac. Sci. Technol. A **3**, 1566 (1985).
[34] T. E. Felter, S. M. Foiles, M. S. Daw, and R. H. Stulen, Surf. Sci. **171**, L379 (1986).
[35] H. Conrad, G. Ertl, J. Küppers, and E. E. Latta, Surf. Sci. **58**, 578 (1976).
[36] J. E. Demuth, Surf. Sci. **65**, 369 (1977).
[37] W. Eberhardt, F. Greuter, and E. W. Plummer, Phys. Rev. Lett. **46**, 1085 (1981).
[38] W. Eberhardt, S. G. Louie, and E. W. Plummer, Phys. Rev. B **28**, 465 (1983).
[39] F. P. Netzer and M. M. El Gomati, Surf. Sci. **124**, 26 (1983).
[40] J. P. Muscat and D. M. Newns, Surf. Sci. **80**, 189 (1979).
[41] J. P. Muscat, Surf. Sci. **110**, 85 (1981).
[42] M. S. Daw and M. I. Baskes, Phys. Rev. B **29**, 6443 (1984).
[43] P. Nordlander, S. Holloway, and J. K. Norskov, Surf. Sci. **136**, 59 (1984).
[44] S. G. Louie, Phys. Rev. Lett. **40**, 1525 (1978).
[45] S. G. Louie, Phys. Rev. Lett. **42**, 476 (1979).
[46] D. Tomanek, S. G. Louie, and C. T. Chan, Phys. Rev. Lett. **57**, 2594 (1986).
[47] D. Tomanek. Z. Sun, and S. G. Louie, Phys. Rev. B **43**, 4699 (1991).
[48] N. A. Baykara, J. Andzelm, D. R. Salahub, and S. Z. Baykata, Int. J. Quantum Chem. **29**, 1025 (1986).
[49] I. Papai, D. R. Salahub, and C. Mijoule, Surf. Sci. **236**, 241 (1990).
[50] M. J. Stott and E. Zaremba, Phys. Rev. B **22**, 1564 (1980).

[51] J. K. Norskov and N. D. Lang, Phys. Rev. B **21**, 2131 (1980).
[52] V. Russier, D. R. Salahub, and C. Mijoule, Phys. Rev. B **42**, 5046 (1990).
[53] D. R. Hamann, J. Electron. Spectrosc. Relat. Phenom. **44**, 1 (1987).
[54] B. Hammer, M. Scheffler, K. W. Jacobsen, and J. K. Norskov, Phys. Rev. Lett. **73**, 1400 (1994).
[55] S. Wilke and M. Scheffler, Surf. Sci. **329**, L605 (1995).
[56] A. Gross, S. Wilke, and M. Scheffler, Phys. Rev. Lett. **75**, 2718 (1995).
[57] B. Hammer and M. Scheffler, Phys. Rev. Lett. **74**, 3487 (1995).
[58] P. Hohenberg and W. Kohn, Phys. Rev. **136**, B864 (1964).
[59] W. Kohn and L. Sham, Phys. Rev. **140**, A1133 (1965).
[60] D. M. Ceperley and B. J. Alder, Phys. Rev. Lett. **45**, 566 (1980).
[61] J. P. Perdew and A. Zunger, Phys. Rev. B **23**, 5048 (1981).
[62] D. Mermin, Phys. Rev. **137**, A1441 (1965).
[63] M. Methfessel and Paxton, Phys. Rev. B **40**, 3616 (1989).
[64] H. J. Monkhorst and J. D. Pack, Phys. Rev. B **13**, 5188 (1976).
[65] R. D. King-Smith, M. C. Payne, and J. S. Lin, Phys. Rev. B **44**, 13 063 (1991).
[66] G. Kresse and J. Hafner, Phys. Rev. B **49**, 14 251 (1994) and (to be published).
[67] J. Furthmüller, G. Kresse, and J. Hafner, Phys. Rev. B **50**, 15 606 (1994).
[68] J. Furthmüller, G. Kresse, and J. Hafner, Europhys. Lett. **28**, 659 (1994).
[69] A. Eichler, J. Hafner, J. Furthmüller, and G. Kresse, Surf. Sci. (to be published).
[70] J. Furthmüller, J. Hafner, and G. Kresse (unpublished).
[71] G. Kresse, Ph.D. Thesis, Technische Universität Wien, 1993.
[72] C. Kittel, *Introduction to Solid State Physics*, 6th ed. (Wiley, New York, 1986).
[73] M. Methfessel, D. Hennig, and M. Scheffler, Phys. Rev. B **46**, 4816 (1992).
[74] O. Bisi and C. Calandra, Surf. Sci. **83**, 83 (1979).